U.S. DEPARTMENT OF COMMERCE
National Oceanic and Atmospheric Administration
Environmental Research Laboratories

NOAA Technical Memorandum ERL NSSL-59

CLOUD-TO-GROUND LIGHTNING VERSUS RADAR REFLECTIVITY IN OKLAHOMA THUNDERSTORMS

Gilbert D. Kinzer

National Severe Storms Laboratory
Norman, Oklahoma
September 1972

TABLE OF CONTENTS

LIST OF FIGURES

LIST OF TABLES

CLOUD-TO-GROUND LIGHTNING VERSUS RADAR REFLECTIVITY IN OKLAHOMA THUNDERSTORMS

Gilbert D. Kinzer
National Severe Storms Laboratory
Norman, Oklahoma

ABSTRACT

Sferic pulse-train amplitudes and arrival times were used to locate lightning flashes and correlate cloud-to-ground lightning with radar reflectivity in two typical Oklahoma storm systems. One system was a squall line lasting about 6 hours and producing detailed azimuthal displays of at least six individual storms with cloud-to-ground lightning. The second system was a group of weaker air mass thunderstorms lasting about 3 hours. Although lightning counts per unit time varied widely between storms and within the same storm, the correlation of lightning counts with the radial extent of radar reflectivity factors $\geq$ 550 mm^6/m^3 was fair. A rough correlation existed between C-G lightning counts and the amount of rainfall. The overall average rate of one cloud-to-ground flash per 1.6×10^{10} g of rainfall found in a limited number of storms compares with Battan's report of one flash per 3×10^{10} g. Even though there was some uncertainty about the rainfall measurements, the Oklahoma results support the opinion that in a developing thunderstorm the number of cloud-to-ground flashes increases more rapidly than the rainfall.

1. INTRODUCTION

Until the destructive effects of cloud-to-ground (C-G) lightning can be mitigated by more positive methods than any now available, early detection and avoidance whenever possible seem to be wise precautions. With this in mind, we studied the radar reflectivity and the location of C-G lightning for two typical groups of Oklahoma storms: one was a squall line and the other an array of air mass storms. A flash is a complete lightning event, either cloud-to-ground, cloud-to-cloud, or a combination of both. In C-G flashes at least one and often several highly luminous return strokes occur during a time of the order of 1 sec in approximately the same channel.

The study attempted to find answers to such questions as: Do reflectivity patterns have characteristics that indicate the existence of C-G lightning? Must a certain level of reflectivity and rainfall rate be exceeded before C-G lightning occurs? How variable is C-G lightning with

respect to the positions of relfectivity centers? Are the total number of C-G flashes for Oklahoma thunderstorms correlated to the total amount of rainfall? Battan, 1965, found this so for thunderstorms occurring over the Catalina Mountains near Tucson, Arizona.

It was desirable to count and locate C-G flashes at ranges extending out as far as 120 n miles. Since the majority of Oklahoma thunderstorms are extensive, rapidly moving, and long lasting, visual sighting such as Battan employed was impractical. An attractive alternative was a somewhat unproved suggestion that the arrival times of pulses in the pulse-trains of sferics provide a measure of the range (Laby et al., 1940; Pierce and Wormell, 1953; and Holzer, 1953). Pulse-trains result from reflections in the waveguide consisting of the lower surface of the ionosphere and the earth's surface, as shown in figure 1. It is only necessary to have a pair of fixed, mutually perpendicular, loop antennas to receive sferic signals, from which we determine the directions of arrival from pulse amplitude ratios and obtain ranges from the timing of the pulses in the trains.

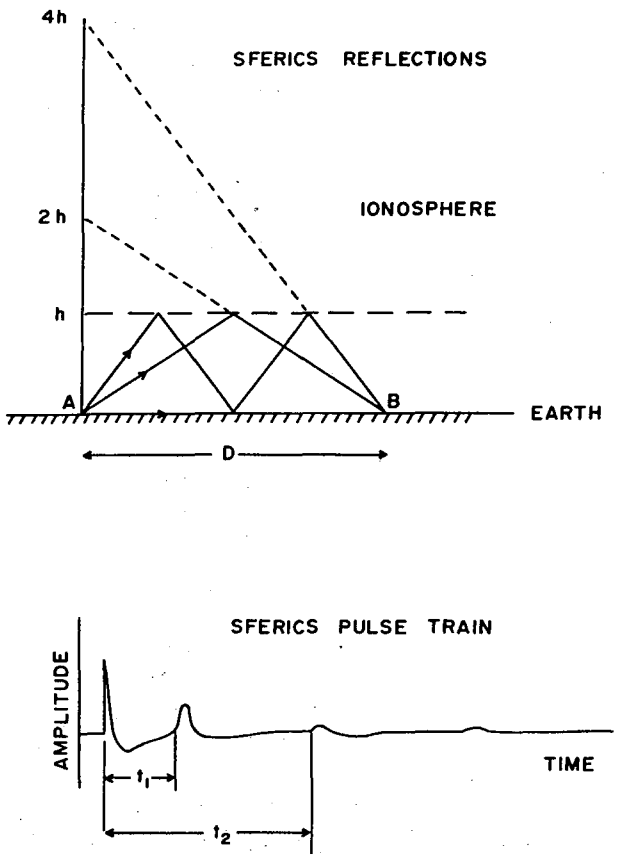

Figure 1. Propagation paths of direct, singly, and multiply reflected sferics from a C-G lightning flash and a sketch of a sferics pulse-train.

The pulse-trains generated by the return stroke components of a C-G flash are predicted fairly well by existing models of lightning and of atmospheric propagation (Bruce and Golde, 1941; Dennis and Pierce, 1964; Uman and McLain, 1969; and Bhattacharya and Rao, 1966). These models show that a sferic pulse travels from the source to a distant observation point along a multiplicity of discrete paths. The shortest path (fig. 1) is along the earth's surface, the next shortest is to the ionosphere for a single reflection back to the observation point; successively longer paths are provided by increasing numbers of reflections between the earth and the ionosphere. The early pulses in a train are pictured in (fig. 1), and the indicated time intervals t_1 and t_2 lead to values for the range, D, and the reflection height, h, given by the equations

$$D = (c/2)\ (t_2^2 - 4t_1^2)\ /\ (4t_1 - t_2) \qquad (1)$$

and

$$h = (c/2)\ (t_1 t_2)^{1/2}\ (t_2 - t_1)^{1/2}\ /\ (4t_1 - t_2)^{1/2}, \qquad (2)$$

where the earth is assumed to be a plane surface and c is the pulse propagation velocity. When the reflection height is known, the range may be obtained more conveniently from the single measurement, t_1, using the equation

$$D = (4h^2 - c^2\ t_1^2)\ /\ 2ct_1. \qquad (3)$$

2. MEASUREMENTS

The WSR-57, 10-cm radar, with its antenna at a 0-degree elevation angle, provided both PPI photographs of contour levels of the integrated video output from a log IF receiver and records of B-scan reflectivity levels whose representations were available from a digital printer. The radar and its signal processing and recording equipment have been described by Sirmans et al., 1970.

The sferic signals were received by two electrostatically shielded, 29-turn, circular loop antennas, 1 m in diameter. One loop was placed north-south in a vertical plane and the other was placed east-west in a vertical plane (fig. 2). After filtering a 60 Hz local signal and wideband voltage amplification, the loop outputs were time integrated to reproduce the waveforms of the received pulses. The amplitudes of the leading pulses of the trains were used for determining azimuth, θ, the tangent of the azimuth of a flash being the ratio of the pulse amplitude from the E-W loop to that from the N-S loop. Figure 3 shows a loop and its associated filter, amplifier, and integrator.

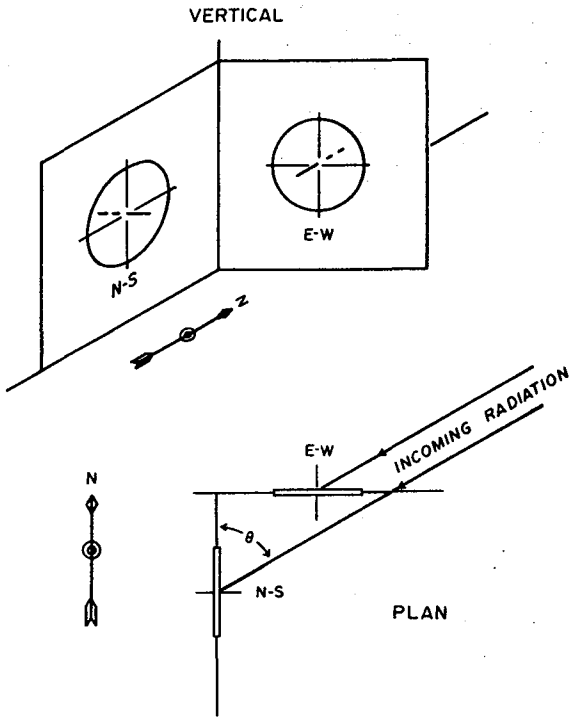

Figure 2. Arrangement of two loop antennas used for locating and counting C-G lightning flashes.

Six display oscilloscopes, used to photograph the sferic pulse-trains, were electrically

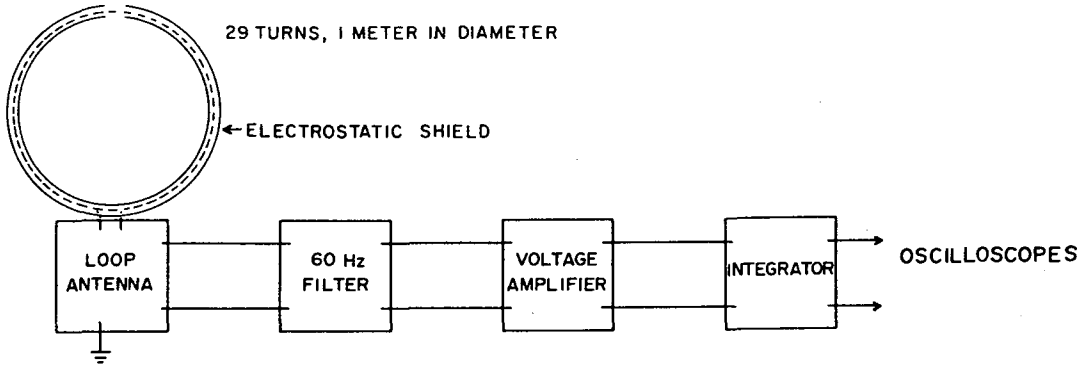

Figure 3. The loop antenna, 60 Hz filter, wideband voltage amplifier, and integrator in the sferics receiver.

interconnected in two rings of three each, one ring for each loop. A small increment of the sweep retrace voltage of an oscilloscope in the first ring triggered the sweep of the next and so on around the ring in unending cycles. The trigger circuits were adjusted so that time lost at each sweep juncture was less than 1 μsec; this provided an almost continuous display of arriving sferics once the sweep cycles were started. The oscilloscopes of the second ring were triggered by those of the first in order to synchronize the two loop records. The arrangement of the oscilloscopes and a recording camera having continuously moving film is shown in figure 4. Considerations of pulse time resolution, spacing

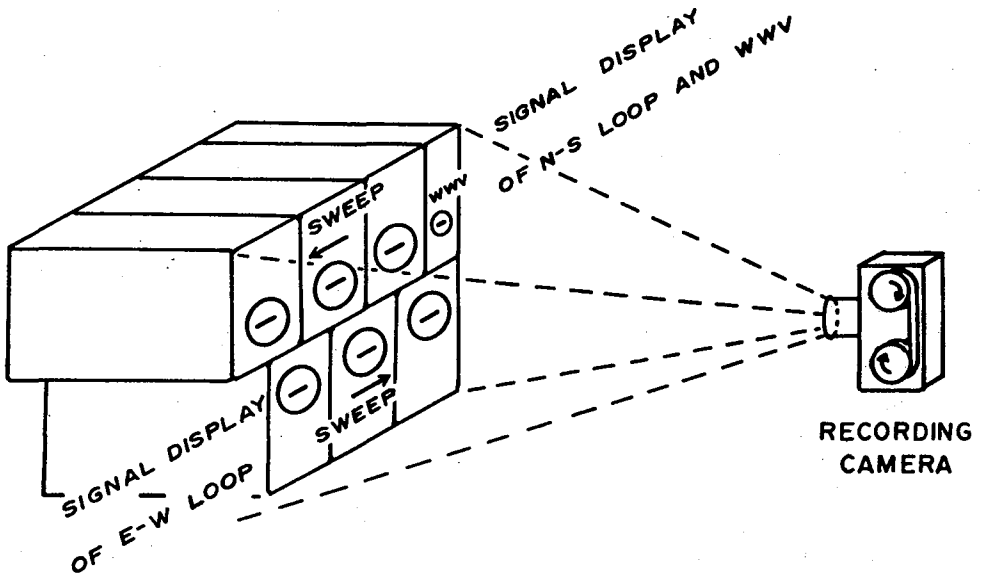

Figure 4. The arrangement of the photographically recording oscilloscopes.

between sweeps, and film bulk dictated 2 msec oscilloscope sweep times, three oscilloscopes per ring, and a film speed of 0.5 cm/sec. Time was recorded by displaying a WWV time signal with an additional oscilloscope. Figure 5 shows samples of typical film records containing corresponding pulse-trains from both loops. These trains, occurring at 2037 CST on June 11, 1969, were generaged by a multiple-return C-G flash that radar showed to be associated with storms in the 4th quadrant approximately 80 n miles away.

Connections to the loop antennas were made so that a C-G return stroke, transferring negative charge to the earth, produced initial polarities of the leading pulses that were related to the quadrant containing the flash, as shown in figure 6. For example, the pulse pairs in figure 5 gave a location in the 4th quadrant at an azimuth of 317 degrees. The corresponding time intervals, t_1 and t_2, were 0.25 and 0.73 msec, respectively; substituting these values into equations (1) and (2) gave a range of 83 n miles and a reflection height of 86 km. The wavy arrow on the PPI photograph (fig. 5) indicates the position of the lightning flash. Of more than 7,000 C-G flashes located by the polarity-quadrant relationships in figure 6, only 14 cases occurred where the location quadrant was opposite to that indicated by radar.

Lightning strokes to the ground have widespread horizontal as well as vertical branching, and a measured location such as that shown on the PPI photograph in figure 5 represents a horizontally weighted position.

As can be seen from the typical pulse-trains in figure 5, the duration of the discernible portion of a train is not likely to exceed 1 msec for the recording gain settings employed in this study. And no cases occurred in which separate trains from a multiple return flash overlapped to such an extent that the timing measurement was uncertain. Furthermore, even when C-G flashes from two or more locations occurred simultaneously the pulses of the two sets of trains could be sorted and measured without difficulty. The reasons for the increasing attenuation of the succeeding pulses in a train are losses due to increasing path lengths, reflection losses, and diminution of intensity for radiation directions approaching that of the return stroke channel, a factor that usually becomes increasingly effective after the first two or three pulses in a train.

At the frequencies that make up the pulse spectra, about 5 kHz to 500 kHz, accepted models of the ionosphere suggest that reflection will occur generally at heights of 70 to 75 km during sunlight and 85 to 90 km at night. The effects of this are shown in figure 7, where two pulse-trains are compared, both coming from a storm approximately 100 n miles away, but with one occurring shortly after midday (1337 CST) and the other occurring at night (2229 CST). The shift from the daytime to the nighttime reflection level increases the magnitudes of both of the time intervals, t_1 and t_2.

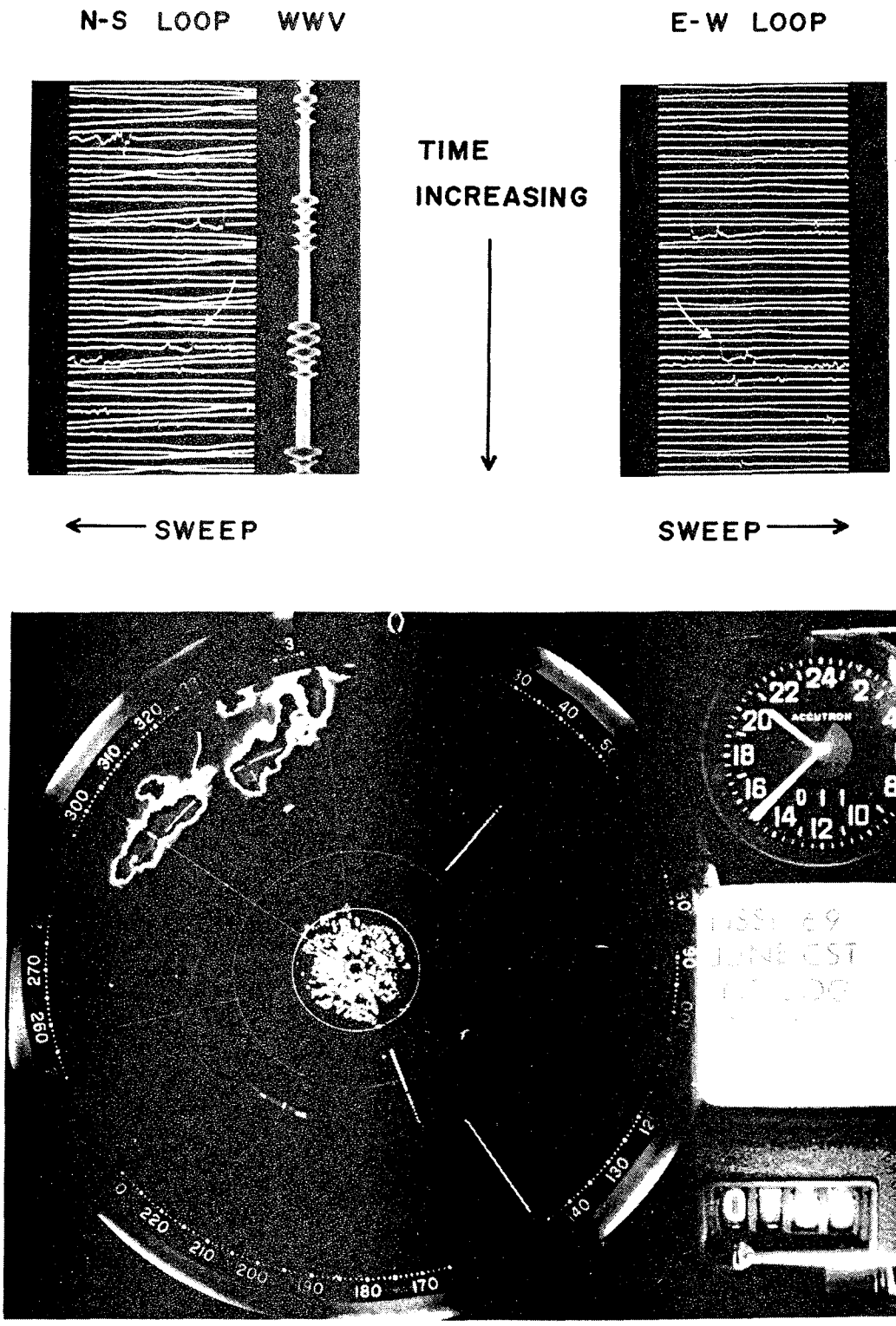

Figure 5. Sample of a pulse-train pair, indicated in the oscilloscope records by curved arrows, and the corresponding lightning flash position indicated in the PPI photograph by a wavy arrow. The oscilloscope sweep time was 2 msec.

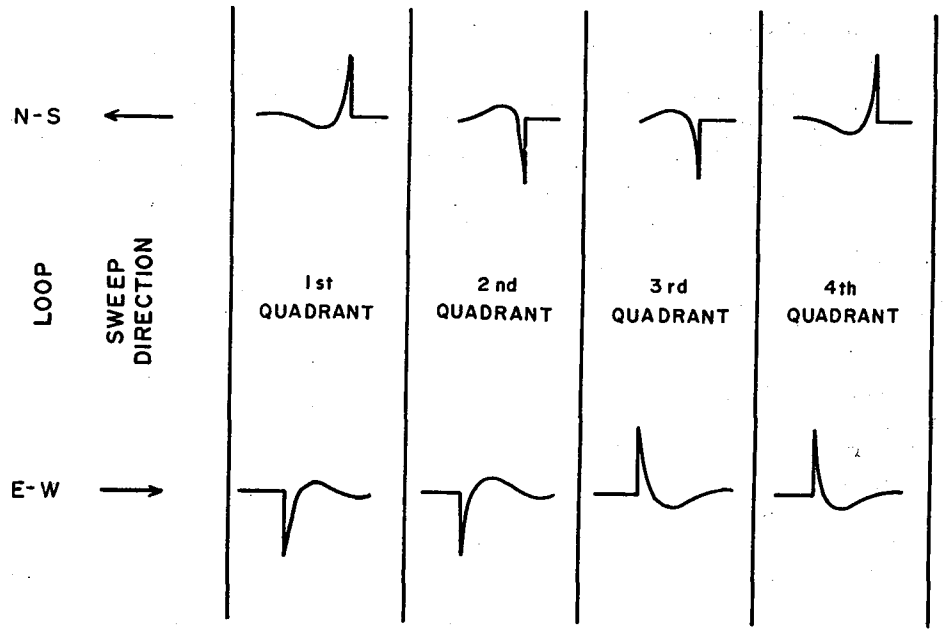

Figure 6. Signal polarities and quadrant locations for a transfer of negative charge to the earth during a C-G flash.

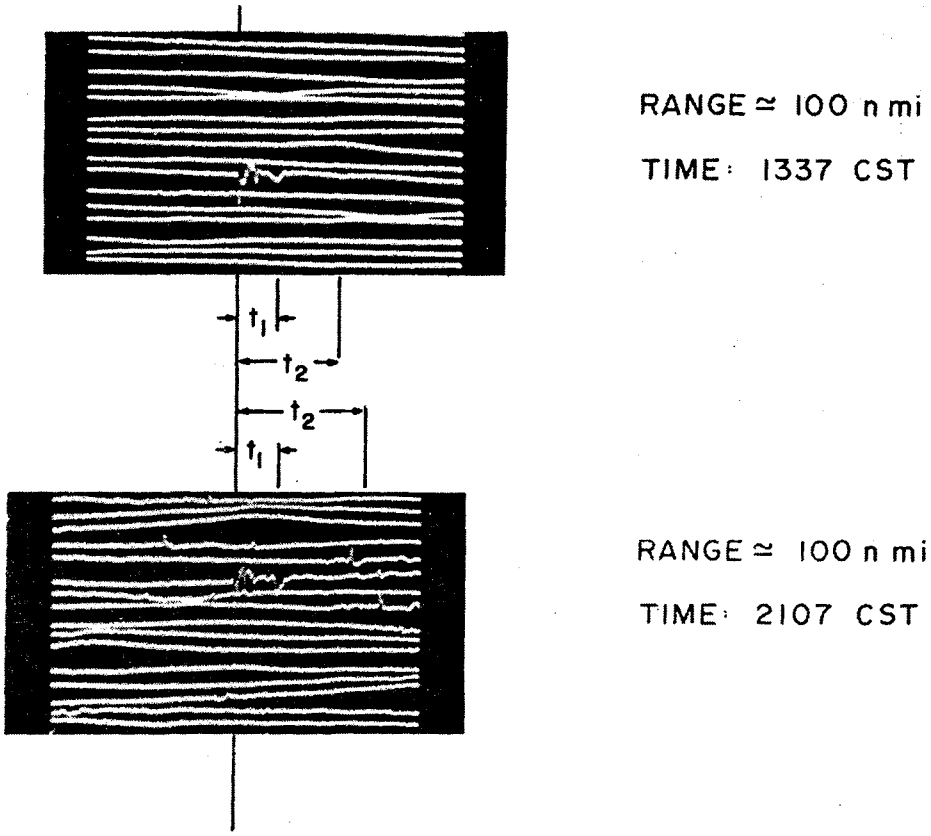

Figure 7. Comparison of daytime and nighttime pulse-trains produced by C-G lightning 100 n miles away.

The timing measurements were employed in the following way: at occsional intervals during a thunderstorm, time increments, t_1, and t_2, were measured using pulse-trains having relatively regular waveforms, and reflection heights were computed to obtain estimates and to uncover any trends of h. Ranges were then obtained using these reflection height estimates, measurements of t_1 and equation (3). The range error, ΔD, resulting from errors Δh and t_1 in h and t_1 may be obtained from the error equation

$$\Delta D = 4h\Delta h/ct_1 - (4h^2 + c^2t_1^2)\, c\Delta t_1 \,/\, 2c^2t_1^2 \,. \qquad (4)$$

Had the pulses approximated the idealized waveforms suggested by the models and pictured qualitatively in figure 1, considerations of time resolution and reading errors would have determined the probable range error. As a matter of fact, observed waveforms usually contained small superimposed irregularities, such as those shown by figure 8, and these irregularities cast doubt over attempts to make precise timing measurements. A subjective judgment allowing for the effects of the irregularities had to be injected into the measurements of t_1 and t_2, creating uncertainties in the range and reflection height that far exceeded those introduced by normal reading errors. At best, it is estimated that the errors in D and h may be as small as $\pm$ 3 n miles and $\pm$ 2 km, respectively; at worst, the errors may be up to five times greater.

Azimuthal errors are produced by several effects: reading errors, sferics polarization, inequalities in the mechanical and electrical aspects of the two loop systems, and radiation distortions produced by nearby unsuspected closed conducting loops. Considerable care was taken to minimize all of the effects except the polarization uncertainties; however, the latter are not believed to be large in the leading nonreflected pulses whose amplitudes provide the azimuth measurements. At most, the azimuthal errors should not exceed 3 degrees.

The three pulse-train samples in figure 9 show empirically observed range effects. With increasing range, the time intervals, t_1 and t_2, diminish, and the initial polarity of the second pulse in a train appears to reverse as shown in figure 10. The waveform positions indicated by the arrows in figure 10 were assumed to be the arrival times at the different ranges.

The measured reflection heights appeared to have a diurnal trend, averaging about 75 km at midday, increasing gradually during the afternoon, becoming as high as 77 km 2 hours before sunset, and reaching 83 km at sunset. During the next 1/2 hour, the reflection height increased to about 86 km, the steady nighttime value, as illustrated by the measurements in figure 11, taken on June 11, 1969, from about an hour before until an hour after sunset. The height variance in figure 11 is typical of measurements of pulse-trains some with and some without the bothersome waveform irregularities discussed earlier.

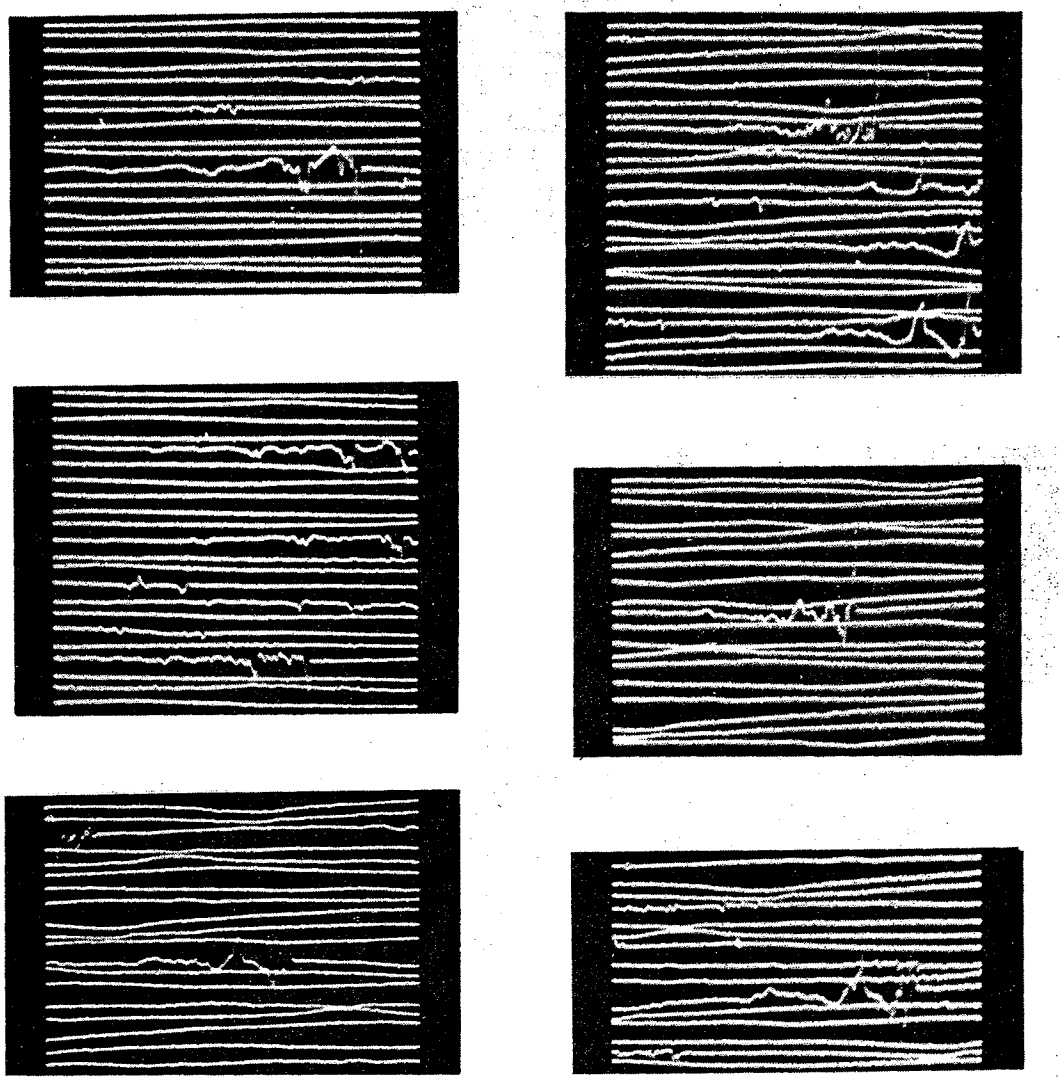

Figure 8. Examples of typical pulse-trains, showing small irregularities superimposed on the general waveform.

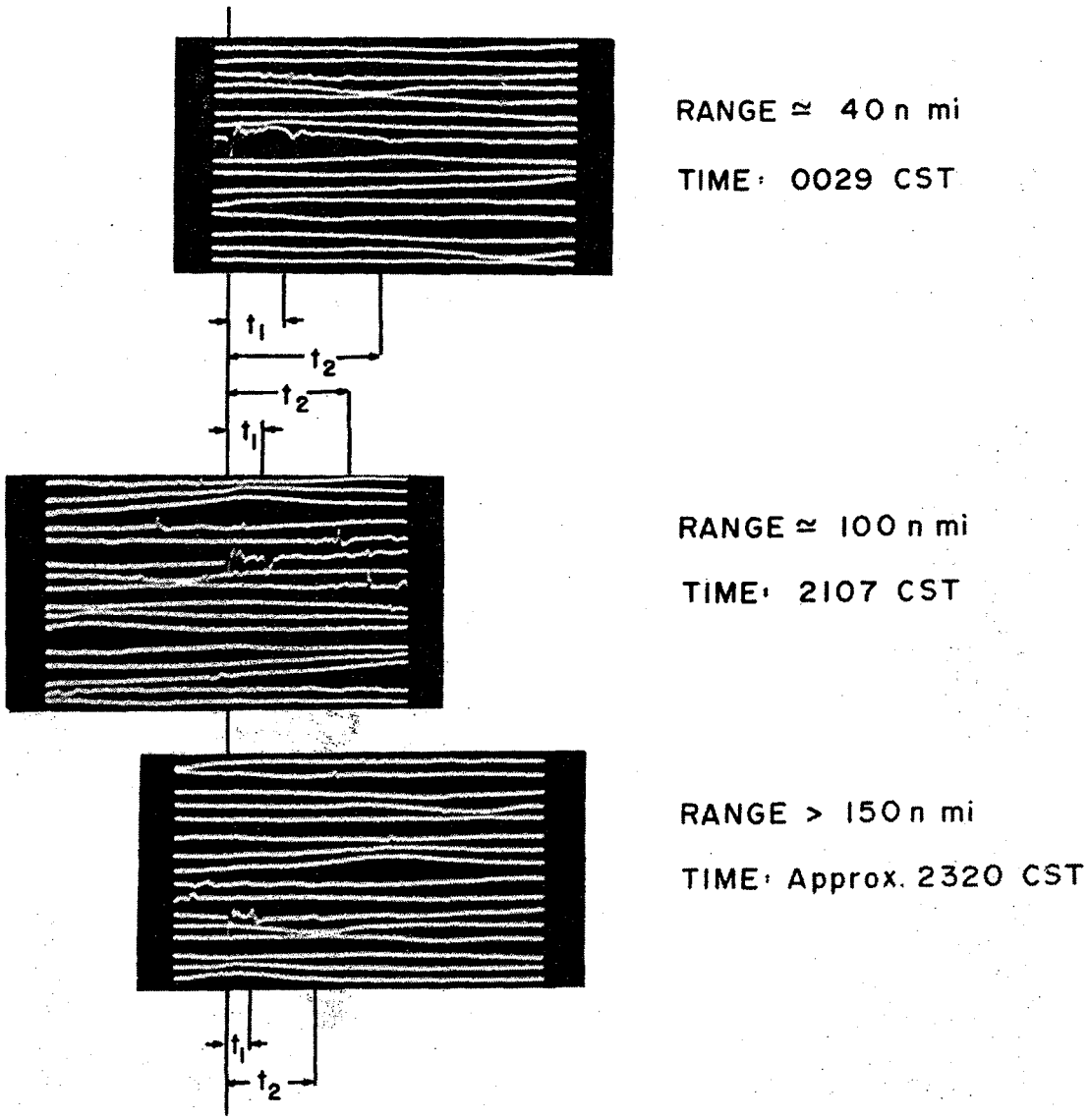

Figure 9. Examples of the effect of range on pulse-trains.

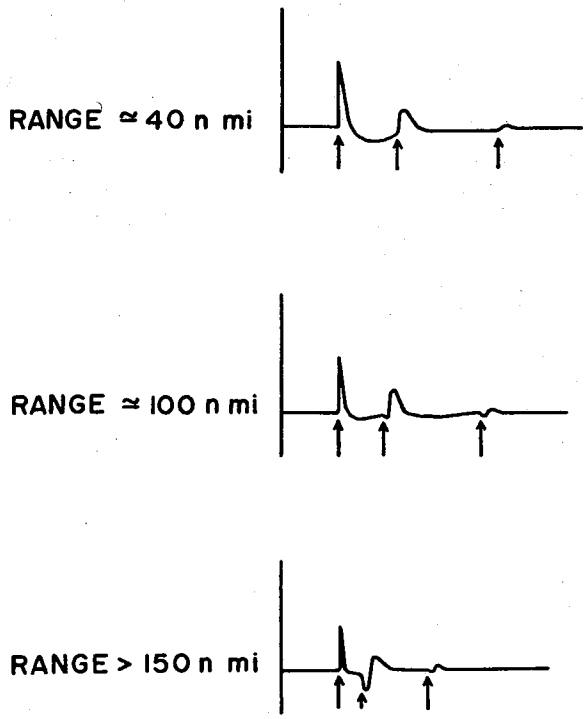

Figure 10. Assumed positions of pulse arrival times.

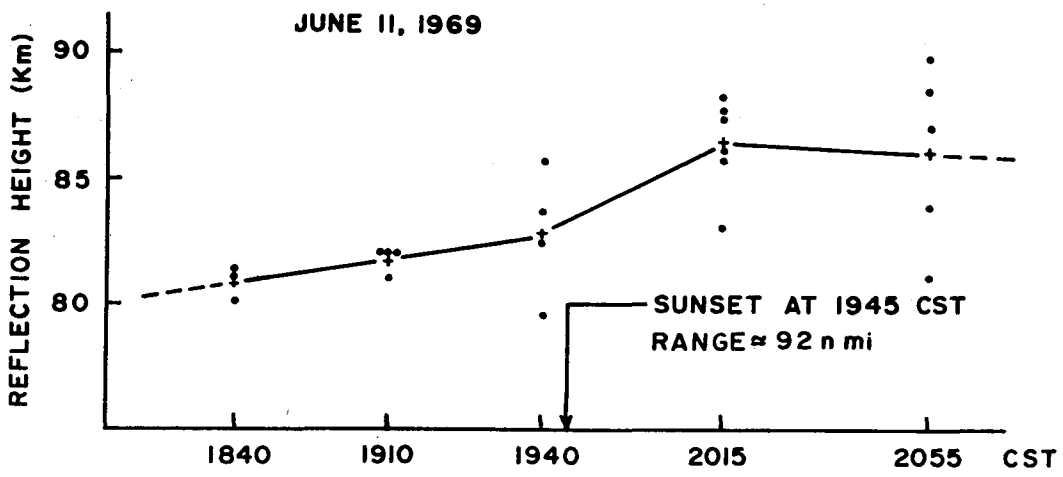

Figure 11. The change in relfection height soon after sunset.

3. CORRELATIONS

On June 11, 1969, a group of storms formed a squall line northwest of Norman, Oklahoma, which persisted from 1805 CST until well beyond 2250 CST, the end of the observing period. The line preceded a slowly moving cold front by about 30 n miles, and this frontal relationship was responsible for the strength and duration of the line. The PPI photograph (fig. 5) shows the line relative to Norman at 2037 CST. The outlines of just detectable reflectivity in figure 12, with superimposed positions of C-G flashes that occurred from 2-1/2 min before the listed times and lasted until 2-1/2 min after, indicate an overall relationship between the lightning and the reflectivity. The line of storms extend as a partial chord across the radar observation circle and furnish a good azimuthal display of lightning and radar reflectivity. The results in figure 12 were derived from 8 out of 45 5-min sferics recordings mostly, although not entirely, consecutive because of the necessity of changing the film about every 35 min.

B-scan reflectivities along each 2-degree radial were recorded every 5 min, and C-G flashes occurring in the 2-degree azimuth intervals bisected by the B-scan radials were counted during 5-min intervals centered on the B-scan times. The digital representation of the B-scan reflectivity shown in figure 13 occurred approximately at the time of the PPI display in figure 5. The reflectivity levels above the peak noise level of the radar were coded from 1 through 9, and translation into return power, $\bar{P}_r$, equivalent radar reflectivity factor, Z, and rainfall rate, r, is shown in table 1.

The first step toward discovering relationships between the reflectivity patterns and the population centers of C-G flashes was to determine how the 5 min lightning counts were distributed with respect to the maximum B-scan level along each scan radial; the results, shown in table 2, lead to the normalized cumulative distributions plotted in figure 14. Most of the C-G flashes appear to be associated with B-scan radials along which the maximum levels are $\geq$ 4 corresponding to a maximum radar reflectivity factor $\geq$ 550 mm^6/m^3. This is more strikingly shown by the fact that of 5594 flashes counted and located during the observations of the squall line only 392 flashes, or about 7 percent, were associated with B-scan maximums $\leq$ 3. In other words, it would have been a good bet that no C-G flashes would occur during a 5-min period, within a 2 degree azimuth interval bisected by a radial along which the radar reflectivity factor was < 550 mm^6/m^3.

The next step was to compare the 5-min counts of C-G flashes to the total radial depth, in n miles, of B-scan levels $\geq$ 4. Typical plots of the paired results are shown in figure 15 for the same set of 5-min observations as in figure 12. There is an appreciable correlation between the extent of rainfall activity represented by the radial depths of reflectivity levels $\geq$ 4, and the C-G lightning activity represented by

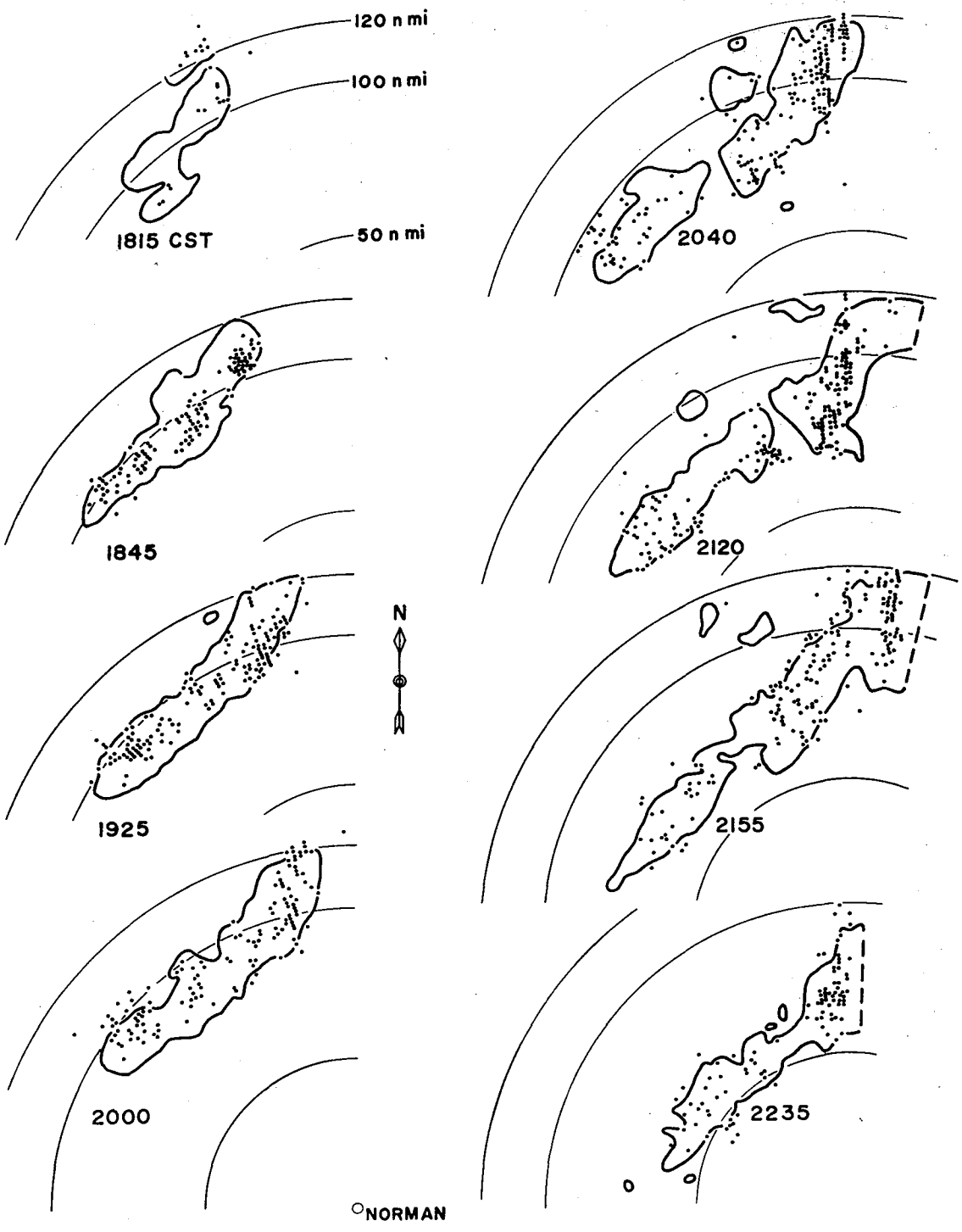

Figure 12. A sequence of radar reflectivity outlines with superimposed positions of 5-min counts of C-G lightning observed for squall line thunderstorms on June 11, 1969.

Table 1. The WSR-57 radar calibration for June 11, 1969, showing the return power, $\bar{P}_r$, the corresponding radar reflectivity factors, Z, and equivalent rainfall rates, r, versus the digitally recorded B-scan reflectivity levels.

Reflectivity Parameter	B-SCAN REFLECTIVITY LEVEL								
	1	2	3	4	5	6	7	8	9
Return power, $\bar{P}_r$ (DBM)	-99	-97	-86	-78	-73	-69	-64	-59	-55
Radar reflectivity factor, $Z(mm^6/m^3)$ *	28	44	550	3,500	11,000	28,000	88,000	280,000	700,000
Equivalent rainfall rate, r(mm/hr) **	0.29	0.39	1.89	6.0	12.3	22	45	92	164

*Range normalized electronically to 100 n miles and mathematically beyond, $Z = \frac{\bar{P}_r \text{ (watts) } R^2}{K^2 \; C}$, R = range in n miles; $C = 4.88 \times 10^{-11}$ (NSSL WSR-57, 10-cm radar); K^2 assumed to be 0.93.

**Marshall-Palmer approximation, $Z = 200r^{1.6}$, used to estimate r.

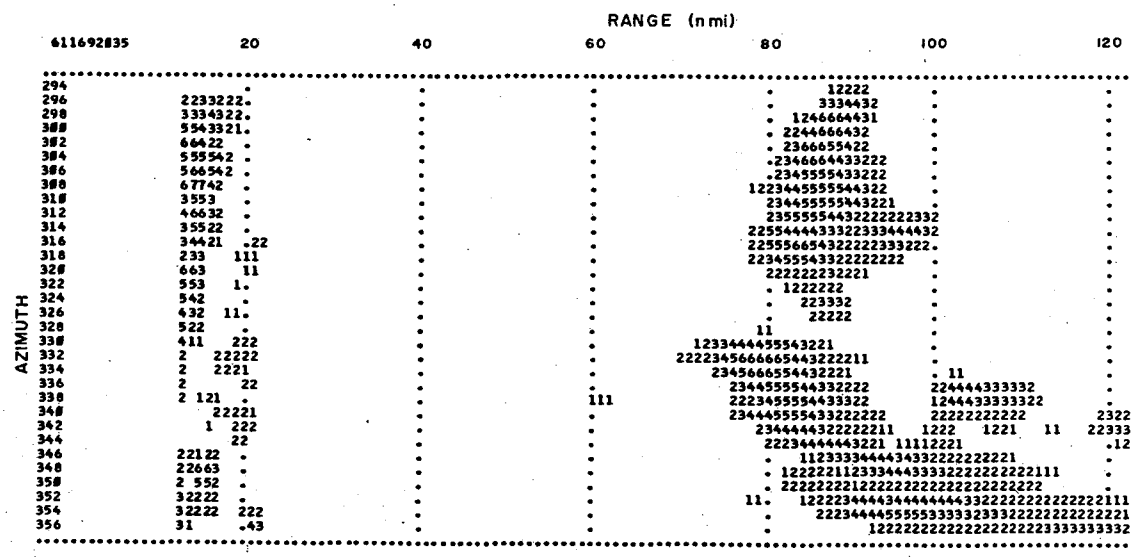

Figure 13. Digital printer representation of horizontal B-scan reflectivity levels corresponding to the PPI photograph in figure 5.

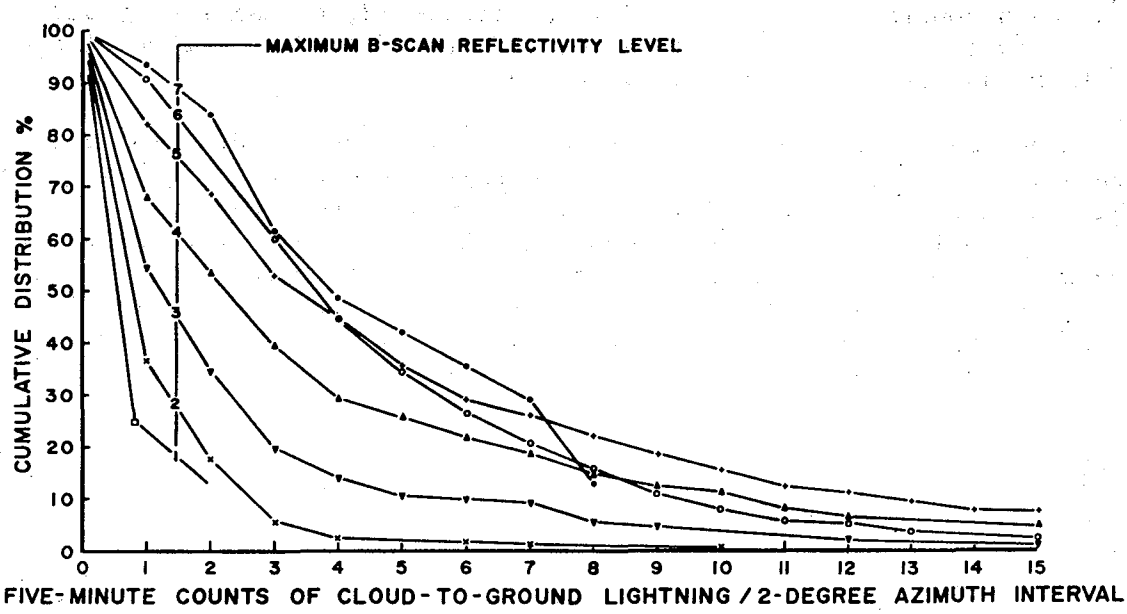

Figure 14. Cumulative distribution of 5-min counts of C-G lightning flashes, occurring in 2-degree azimuth intervals, as a function of the maximum B-scan reflectivity levels along radials bisecting the azimuth intervals.

Table 2. Bivariate frequency table of 5-min counts of C-G flashes, occurring in 2-degree azimuth intervals, versus maximums of B-scan reflectivity levels along radials bisecting the azimuth intervals.

Maximum B-Scan Reflectivity Level	FIVE-MINUTE COUNTS OF CLOUD-TO-GROUND LIGHTNING PER 2-DEGREE AZIMUTH INTERVAL																													
	0	1	2	3	4	5	6	7	8	9	10	11	12	13	14	15	16	17	18	19	20	21	22	23	24	27	28	29	33	34	38
0	6	11	2																												
1	18	3	3																												
2	111	33	21	6	1		1	1			1																				
3	64	28	21	8	5	1	1	5	1	4			1			1		1													
4	104	48	45	34	11	13	10	12	8	4	10	6	5			1	1	1	2	1	2	1	1		3		1		1	1	
5	99	73	86	46	51	33	17	21	19	17	18	6	9	8	3	9	5	3	3	3	6		4		2	1	2	1			1
6	29	47	49	48	32	25	18	16	14	9	7	2	5	4		2	2	1		1		1			1						
7	2	3	7	4	2	2	2	5	4					1																	

C-G flash counts. But figure 15, like figure 12, contains only about one-sixth of the total measurements; therefore, another method of comparison was devised for the complete set.

The radial depth of B-scan levels ≥ 4 was contoured on the relief map shown in figure 16, having azimuth-time coordinates. The ridges on this map indicate both individual storm centers and their azimuthal movement; the valleys marked by dashed lines between the ridges represent zones of reduced or negligible rainfall. The trapezoidal outline of the map arises from two circumstances: first, the length of the squall line increased with time, and second, the line drifted slowly southeast toward Norman, as shown in figure 12. Note that the area shown by the left side

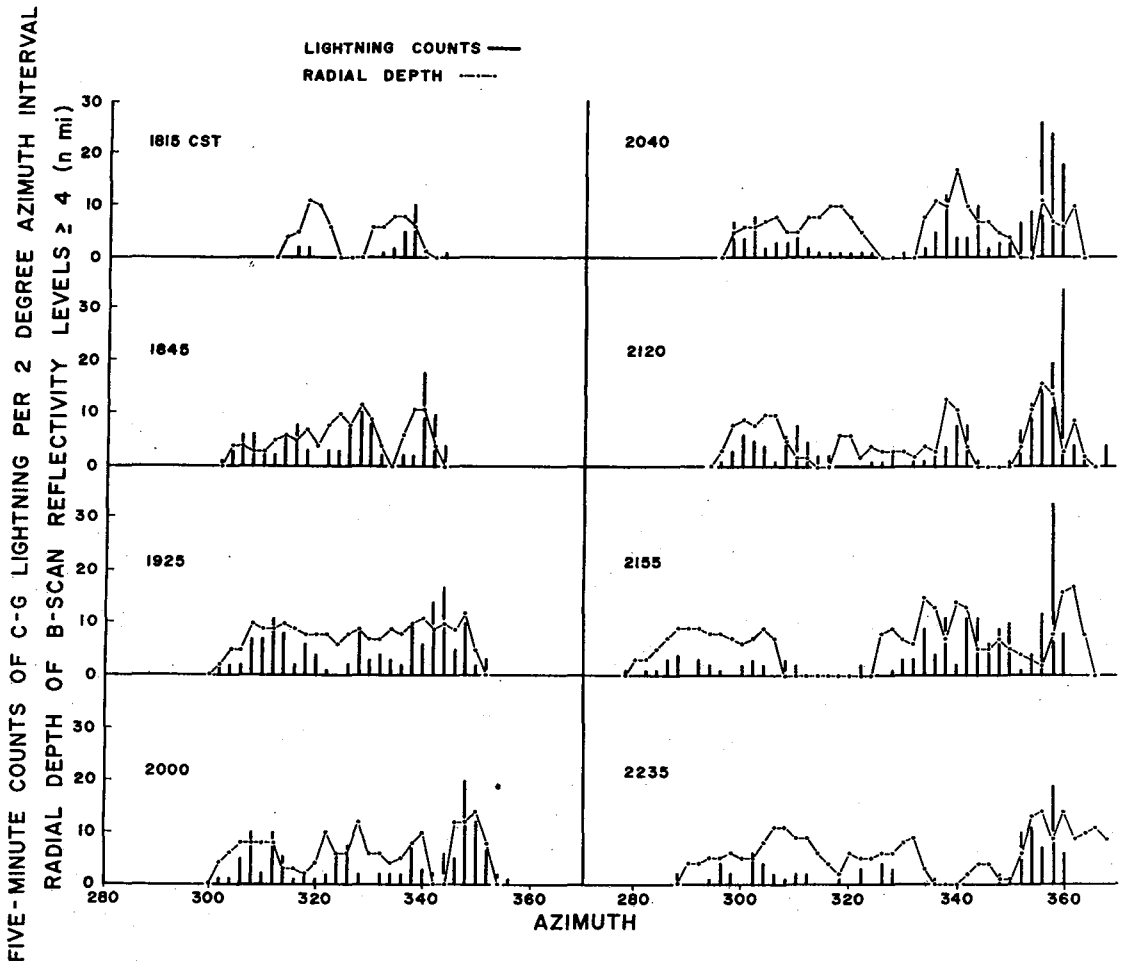

Figure 15. Azimuthal distributions of 5-min counts of C-G lightning flashes occurring in 2-degree azimuth intervals and of the depth in n miles of B-scan levels ≥ 4 along radials bisecting the azimuth intervals.

of the map was a breeding zone from which storms disengaged themselves and moved to the right.

Another map, figure 17, was constructed showing the counts of C-G lightning flashes with the valley traces of figure 16 superimposed. These traces are centered on regions of minimum counts and appear to separate the heights of lightning activity quite well. It is easy to see that azimuth and time of occurrence correlate well between the two maps.

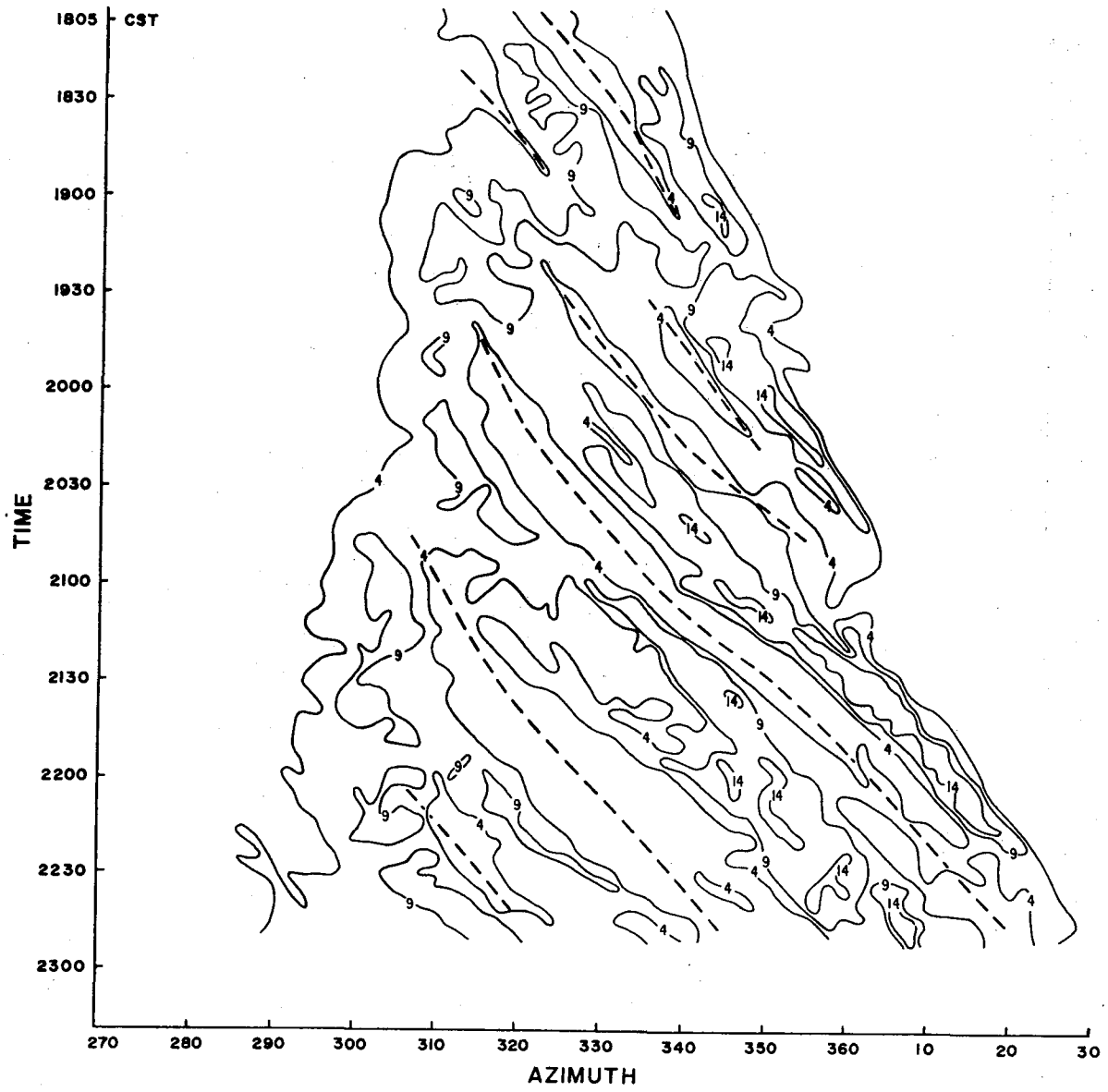

Figure 16. Contours of the depth in n miles of B-scan reflectivity levels on an azimuth-time coordinate map.

However, the correlation of numbers of flashes with radial depth of B-scan reflectivities ≥ 4 appears to be somewhat nonlinear, the flash counts increasing more rapidly. Table 3 shows bivariate frequency distribution of pairs of values of radial depths and flash counts, taken from figures 16 and 17, and, because of large variances and the nonlinear tendency, the linear correlation ratio is only 0.38.

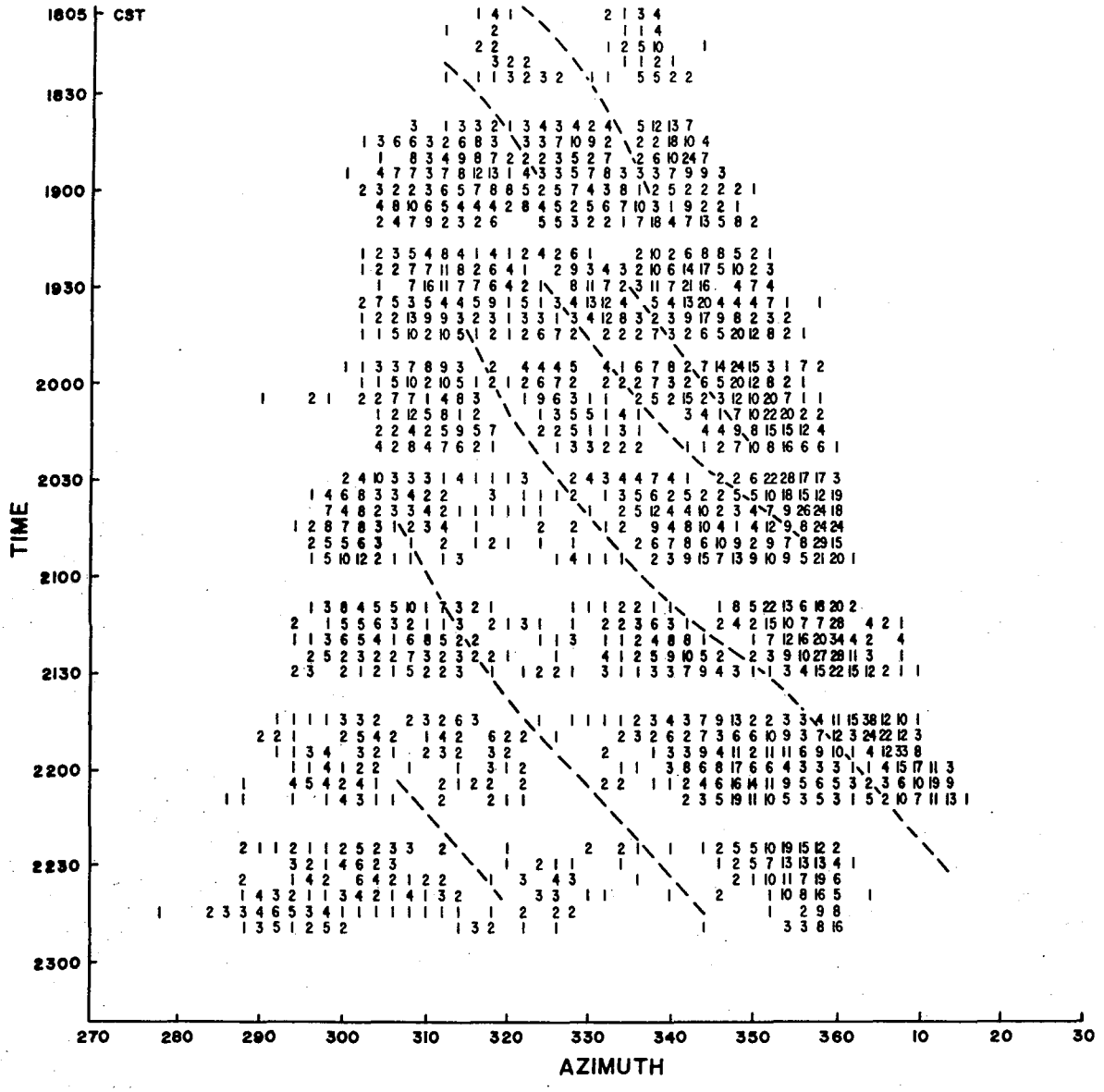

Figure 17. Map of 5-min counts of C-G lightning flashes occurring in 2-degree azimuth intervals.

Table 3. Bivariate frequency table of 5-min counts of C-G flashes occurring in 2-degree azimuth intervals, versus depth in n miles of B-scan reflectivity levels ≥ 4 along radials bisecting the azimuth intervals.

Radial Depth of B-Scan Levels ≥ 4 (n mi)	FIVE-MINUTE COUNTS OF CLOUD-TO-GROUND LIGHTNING PER 2-DEGREE AZIMUTH INTERVAL																														
	0	1	2	3	4	5	6	7	8	9	10	11	12	13	14	15	16	17	18	19	20	21	22	23	24	27	28	29	33	34	38
0	90	73	47	14	7	1	2	7	1	4	1		1			1		1													
1	16	2	1	2			1		1				1																		
2	27	12	12	6	4	3		2	2		1	1	1	1		1							1		1						
3	34	20	17	14	4	3	4	4			1	1		1											1					1	
4	39	23	15	10	7	2	3	2	3	2	1								1		1	1									
5	21	18	22	16	7	6	5	4	5	1	4	1																			
6	33	21	23	17	13	6	6	5	5	2	5	1	1					1	1												
7	17	23	24	19	12	8	1	3	7	6	3	2	1	1			1				1				1						1
8	16	26	23	12	15	13	4	12	7	2	6			1		2			1				1		1			1	1		
9	14	12	19	17	11	14	3	3	5	6	1	2	6	1	1	2	1	1		1							1				
10	9	8	10	10	11	6	7	6	3	2	5	1	3	1			2	1							1		1				
11	5	6	11	6	4	7	5	6	2	3	2	1	1	1	1	1	2	1	1		1										
12	1	1	4		2	3	2	1		2	2		1	2		2	1	1	1	3	2	1	1								
13	1		1	1	4	1	1	4		2	1	2	1	1		2				1	2										
14	1		2			1	4	1	3			1	1	2	1						1					1					
15			3						1	1	1	1		1		1							1		1						
16				1			1		1	1	2						1						1								
17	2	1		1	1											1											1				
18													1																		
19													1																		

Rather than search for more details of correlation between figures 16 and 17, we directed our attention to the question: What rainfall amount, on the average, is associated with a C-G flash? Figure 16 shows seven separate storm areas, between the valley traces. The amount of rainfall in each 5-min interval was estimated from the B-scan reflectivities for each of the storm centers in figure 16 using the calibration given in table 1. At corresponding 5-min intervals, the lightning flash counts for each storm were accumulated also, and the paired results were plotted logarithmically in figure 18 for comparison with results that Battan (1965) obtained from thunderstorms over the Catalina Mountains near Tucson, Arizona. Battan's data, not reproduced here, represented daily measurements for 52 stormy days and had a greater range of values with about the same degree of scatter. He represented his data with a line, reproduced in figure 18; although the line possibly represents the present measurements, a position farther to the left would be better. Battan estimated that 3×10^{10} g of rain fell, on the average, per C-G lightning flash compared with 1.6×10^{10} g per flash estimated for the June 11th Oklahoma squall line storms. These differences could be due to the natural variability in thunderstorms and the limited number of storms in the present study. On the other hand, it seems reasonable to suspect

that the large and long-lasting storms of the plains may produce C-G lightning more effectively than mountain storms. Battan pointed out that his surface measurements of rainfall did not allow for evaporative loss while the precipitation was falling; the same is true of rainfall amounts given in this study, since the empirical relationship used for converting reflectivity to rainfall rates in table 1 was developed from surface rain measurements.

On May 14, 1969, a group of thunderstorms formed a broad north-south band east of Norman and produced the reflectivity displays of the type shown in figure 19. These were air mass thunderstorms, individually short-lived and widely dispersed. They showed little movement in contrast to the storms making up the June 11th squall line. Several 5 min counts of C-G flashes and corresponding rainfall amounts estimated from B-scan reflectivities were obtained for individual storms of this second group, and the results, shown as triangles in figure 18, fall close to a mean position of the points derived for the June 11th storms.

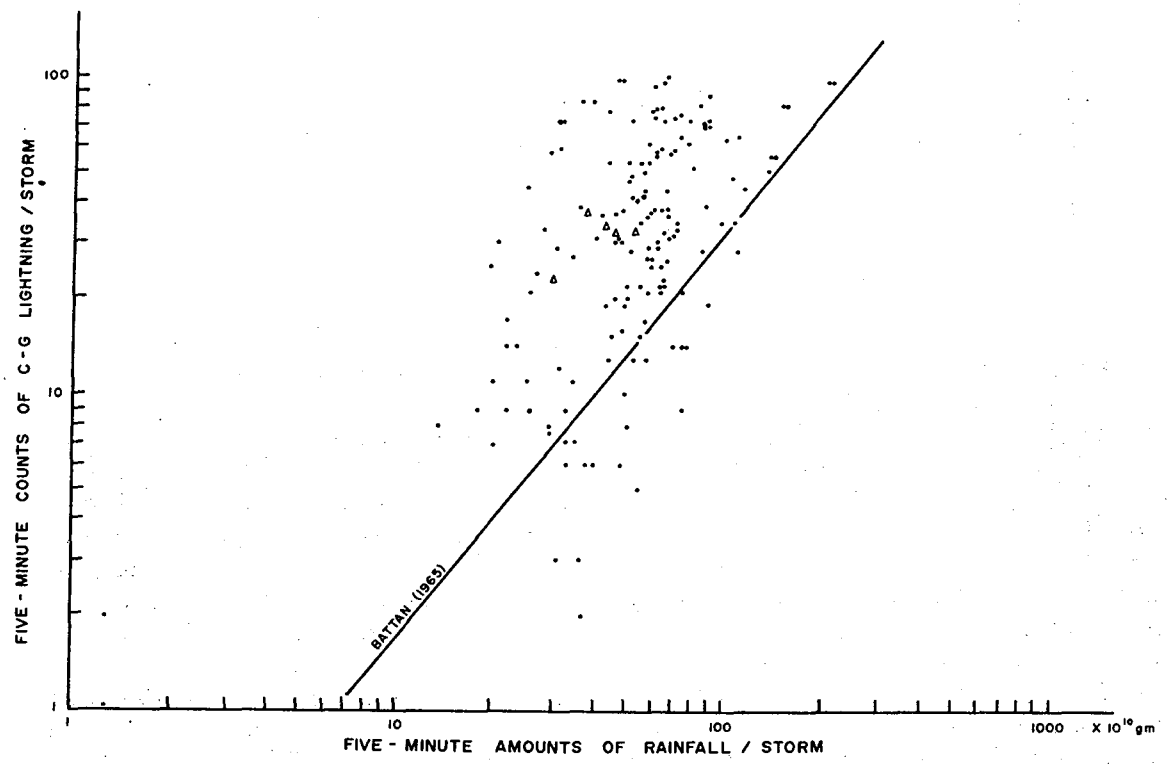

Figure 18. Logarithmic plot of 5-min counts of C-G flashes per storm versus corresponding 5-min rainfall amounts per storm for the June 11th squall line. The inclined line is a representation given by Battan (1965) for thunderstorms over the Catalina Mountains near Tucson, Arizona. The points shown as small triangles were obtained from the air mass storms of May 14th shown in figure 19.

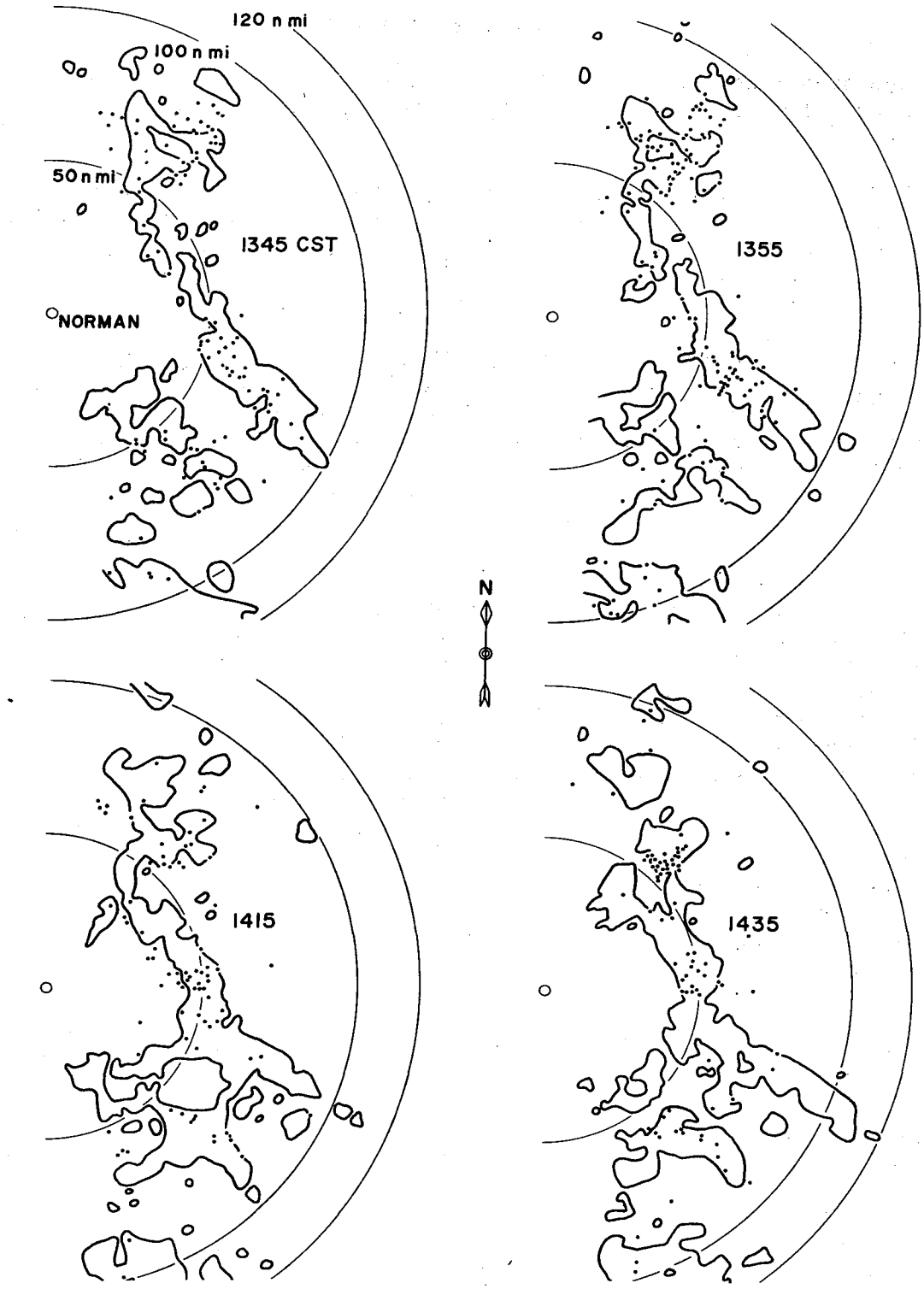

Figure 19. A sequence of radar reflectivity outlines with superimposed positions of 5-min counts of C-G lightning flashes observed for a group of air mass thunderstorms on May 14, 1969.

4. CONCLUDING REMARKS

The questions raised in the introduction cannot be answered completely from a limited sample of Oklahoma storms, but partial answers can be suggested.

What is the nature of the correlation between radar reflectivity and C-G lightning? An examination of figures 16 and 17 suggest that areas of greater reflectivity are apt to be areas of higher rates of C-G lightning and that, on the average, the lightning activity increases rapidly with the increase in the radial depth of reflectivity.

Was there a radar reflectivity factor threshold for the occurrence of C-G lightning? The answer could be a qualified yes; the threshold being about 550 mm^6/m^3 when larger reflectivities exist in nearby storm centers, or when the growth rate of new areas of reflectivity suggests that ultimate values are likely to exceed this amount. Table 2 and figure 14 show that the threshold is not sharp, since C-G lightning occurred occasionally at smaller reflectivities.

How variable is C-G lightning with respect to areas of reflectivity? First of all, in the well-organized squall line C-G flashes showed a strong tendency to occur inside areas of reflectivity. Judging from figure 12, for example, at least nine out of every ten C-G flashes occurred inside areas of reflectivity, for the June 11th storms. Most cases when the C-G flashes were outside reflective areas appeared to result from a displacement in range rather than azimuth, and we suspect that the errors in range measurements caused by the irregularities of the pulse shapes were responsible. On the other hand, only about six out of ten flashes associated with the air mass thunderstorms of May 14th occurred inside reflectivity areas, see figure 19. Although these two sets of observations alone do not furnish meaningful statistics about Oklahoma thunderstorms, they do conform with the impression, gained from many visual observations, that C-G lightning in squall line thunderstorms is much more compact than in air mass thunderstorms.

Is the number of C-G lightning flashes occurring in Oklahoma squall line thunderstorms correlated with the amount of rainfall, as reported by Battan (1965) for thunderstorms over the Catalina Mountains near Tucson, Arizona? The measurements in figure 18 indicate that about the same extent of correlation exists, and 1.6×10^{10} g of rainfall per C-G flash, on the average, for the Oklahoma storms agrees within an order of magnitude of the 3×10^{10} g per C-G flash reported by Battan. This agreement may be somewhat fortuitous, since the number of Oklahoma storms measured was too limited to represent an adequate sample, and the radar estimates of rainfall amounts had some uncertainties. The most important correlation feature suggested by both studies is a disproportionately greater increase in the number of C-G flashes when the rainfall amount increases.

What about the feasibility of using sferic pulse-trains from stroke components of C-G lightning flashes for locating and counting the flashes within radar range? Mutually perpendicular and well-matched loop antennas, each with its own receiving and recording channel, furnished well-resolved pulse-trains from which the azimuths were obtained with an uncertainty estimated to be less than 3 degrees. Interpretations of time intervals between successive pulses in a train furnished C-G lightning ranges agreeing approximately with radar indicated storm positions and gave reasonable estimates of ionospheric reflection heights. Inherent irregularities in the pulse waveforms interfered with the timing measurements enough to introduce range uncertainties that could be as large as 15 n miles over a radar range of 120 n miles, and this prohibited correlation studies between small-scale features of C-G lightning distributions and precipitation reflectivity patterns. For the storms sampled during this study, the assumption that the return stroke transferred negative electricity to the earth led to an interpretation of the observed polarity of the initial portion of the first pulse in a pulse train that almost always positioned the flash in the storm quadrant indicated by radar.

The sferic records were excellent for counting C-G lightning flashes associated with storms occurring between 35 to 120 n miles. Counts at other ranges were limited only by the observer's ability to recognize and sort sferic pulse-trains. Even for storms having a high amount of lightning activity, no difficulty was experienced in identifying individual pulse-trains and in locating and counting flashes. Although it is conceivable that the amplitude of a pulse-train might be too small to properly measure, none appeared to be this way within radar range, possibly because C-G flashes are disruptive processes that occur only when the effective breakdown strength of the atmosphere is exceeded and establish a minimum signal strength that is adequately recorded when the system gain is adjusted for thunderstorms in a 35 to 120 n mile range.

Cloud-to-ground lightning may be closely related to storm features that are not shown in PPI and B-scan reflectivity patterns. It would be surprising, for example, if the rate and extent of vertical development of reflectivity and of air circulation within the storm were unimportant. But these processes occur at scales that probably are smaller than the uncertainties in position measurements attainable from sferic pulse-trains, and no attempt was made to consider them. Similarly, temporal variations of C-G flashes over time spans of less than 5 min were not considered either, although the timing of flash components within $\pm$ 1 msec was possible. This kind of information will become more important when lightning flashes can be more accurately located relative to the dynamical storm processes.

5. REFERENCES

Battan, L. J., 1965: Some factors governing precipitation and lightning in convective clouds. J. Atmos. Sci., 22, 79-84.

Bhattacharya, H. and M. Rao, 1966: Effect of ionospheric reflections on the nature of the wave forms of radio atmospherics. Radio-Sci., 1, 309-312.

Bruce, C. E. R. and R. H. Golde, 1941: The lightning discharge. J. IEEE London, 88, 487-524.

Dennis, A. S. and E. T. Pierce, 1964: The return stroke of a lightning flash to earth as a source of ULF atmospherics. Radio Sci., 68D, 777-794.

Holzer, R. E., 1953: Simultaneous measurement of sferics signals and thunderstorm activity. Thunderstorm Electricity, ed. R. H. Byers, University of Chicago Press, Chapter 13.

Laby, T. H., J. J. McNeill, F. G. Nicholls and A. F. B. Nickson, 1940: Waveform, energy and reflection by the ionosphere, of atmospherics. Proc. Roy. Soc. London, Ser. A 174, 145-163.

Pierce, E. T. and T. W. Wormell, 1953: Field changes due to lightning discharges. Thunderstorm Electricity, ed. R. H. Byers, University of Chicago Press, Chapter 12.

Sirmans, D., W. L. Watts and J. H. Horwedel, 1970: Weather radar signal processing and recording at the National Severe Storms Laboratory. IEEE Trans. on Geosci. Electronics GE-8, 88-94.

Uman, M. A. and D. K. McLain, 1969: Magnetic field of the lightning return stroke. J. Geophys. Res., 74, 6899-6909.

NATIONAL SEVERE STORMS LABORATORY

The NSSL Technical Memoranda, beginning with No. 28, continue the sequence established by the U. S. Weather Bureau National Severe Storms Project, Kansas City, Missouri. Numbers 1-22 were designated NSSP Reports. Numbers 23-27 were NSSL Reports, and 24-27 appeared as subseries of Weather Bureau Technical Notes. These reports are available from the National Technical Information Service, Operations Division, Springfield, Virginia 22151, for $3.00, and a microfiche version for $0.95. NTIS numbers are given below in parentheses.

No. 1 National Severe Storms Project Objectives and Basic Design. Staff, NSSP. March 1961. (PB-168207)

No. 2 The Development of Aircraft Investigations of Squall Lines from 1956-1960. B. B. Goddard. (PB-168208)

No. 3 Instability Lines and Their Environments as Shown by Aircraft Soundings and Quasi-Horizontal Traverses. D. T. Williams. February 1962. (PB-168209)

No. 4 On the Mechanics of the Tornado. J. R. Fulks. February 1962. (PB-168210)

No. 5 A Summary of Field Operations and Data Collection by the National Severe Storms Project in Spring 1961. J. T. Lee. March 1962. (PB-165095)

No. 6 Index to the NSSP Surface Network. T. Fujita. April 1962. (PB-168212)

No. 7 The Vertical Structure of Three Dry Lines as Revealed by Aircraft Traverses. E. L. McGuire. April 1962. (PB-168213)

No. 8 Radar Observations of a Tornado Thunderstorm in Vertical Section. Ralph J. Donaldson, Jr. April 1962. (PB-174859)

No. 9 Dynamics of Severe Convective Storms. Chester W. Newton. July 1962. (PB-163319)

No. 10 Some Measured Characteristics of Severe Storms Turbulence. Roy Steiner and Richard H. Rhyne. July 1962. (N62-16401)

No. 11 A Study of the Kinematic Properties of Certain Small-Scale Systems. D. T. Williams. October 1962. (PB-168216)

No. 12 Analysis of the Severe Weather Factor in Automatic Control of Air Route Traffic. W. Boynton Beckwith. December 1962. (PB-168217)

No. 13 500-Kc./Sec. Sferics Studies in Severe Storms. Douglas A. Kohl and John E. Miller. April 1963. (PB-168218)

No. 14 Field Operations of the National Severe Storms Project in Spring 1962. L. D. Sanders. May 1963. (PB-168219)

No. 15 Penetrations of Thunderstorms by an Aircraft Flying at Supersonic Speeds. G. P. Roys. Radar Photographs and Gust Loads in Three Storms of 1961 Rough Rider. Paul W. J. Schumacher. May 1963. (PB-168220)

No. 16 Analysis of Selected Aircraft Data from NSSP Operations, 1962. T. Fujita. May 1963. (PB-168221)

No. 17 Analysis of Methods for Small-Scale Surface Network Data. D. T. Williams. August 1963. (PB-168222)

No. 18 The Thunderstorm Wake of May 4, 1961. D. T. Williams. August 1963. (PB-168223)

No. 19 Measurements by Aircraft of Condensed Water in Great Plains Thunderstorms. George P. Roys and Edwin Kessler. July 1966. (PB-173048)

No. 20 Field Operations of the National Severe Storms Project in Spring 1963. J. T. Lee, L. D. Sanders and D. T. Williams. January 1964. (PB-168224)

No. 21 On the Motion and Predictability of Convective Systems as Related to the Upper Winds in a Case of Small Turning of Wind with Height. James C. Fankhauser. January 1964. (PB168225)

No. 22 Movement and Development Patterns of Convective Storms and Forecasting the Probability of Storm Passage at a Given Location. Chester W. Newton and James C. Fankhauser. January 1964. (PB-168226)

No. 23 Purposes and Programs of the National Severe Storms Laboratory, Norman, Oklahoma. Edwin Kessler. December 1964. (PB-166675)

No. 24 Papers on Weather Radar, Atmospheric Turbulence, Sferics, and Data Processing. August 1965. (AD-621586)

No. 25 A Comparison of Kinematically Computed Precipitation with Observed Convective Rainfall. James C. Fankhauser. September 1965. (PB-168445).

No. 26 Probing Air Motion by Doppler Analysis of Radar Clear Air Returns. Roger M. Lhermitte. May 1966. (PB-170636)

No. 27 Statistical Properties of Radar Echo Patterns and the Radar Echo Process. Larry Armijo. May 1966. The Role of the Kutta-Joukowski Force in Cloud Systems with Circulation. J. L. Goldman. May 1966. (PB-170756)

No. 28 Movement and Predictablity of Radar Echoes. James Warren Wilson. November 1966. (PB-173972)

No. 29 Notes on Thunderstorm Motions, Heights, and Circulations. T. W. Harrold, W. T. Roach, and Kenneth E. Wilk. November 1966. (AD-644899)

No. 30 Turbulence in Clear Air Near Thunderstorms. Anne Burns, Terence W. Harrold, Jack Burnham, and Clifford S. Spavins. December 1966. (PB-173992)

No. 31 Study of a Left-Moving Thunderstorm of 23 April 1964. George R. Hammond. April 1967. (PB-174681)

No. 32 Thunderstorm Circulations and Turbulence from Aircraft and Radar Data. James C. Fankhauser and J. T. Lee. April 1967. (PB-174860)

No. 33 On the Continuity of Water Substance. Edwin Kessler. April 1967. (PB-175840)

No. 34 Note on the Probing Balloon Motion by Doppler Radar. Roger M. Lhermitte. July 1967. (PB-175930)

No. 35 A Theory for the Determination of Wind and Precipitation Velocities with Doppler Radars. Larry Armijo. August 1967. (PB-176376)

No. 36 A Preliminary Evaluation of the F-100 Rough Rider Turbulence Measurement System. U. O. Lappe. October 1967. (PB-177037)

No. 37 Preliminary Quantitative Analysis of Airborne Weather Radar. Lester P. Merritt. December 1967. (PB-177188)

No. 38 On the Source of Thunderstorm Rotation. Stanley L. Barnes. March 1968. (PB-178990)

No. 39 Thunderstorm - Environment Interactions Revealed by Chaff Trajectories in the Mid-Troposphere. James C. Fankhauser. June 1968. (PB-179659)

No. 40 Objective Detection and Correction of Errors in Radiosonde Data. Rex L. Inman. June 1968. (PB-180284)

No. 41 Structure and Movement of the Severe Thunderstorms of 3 April 1964 as Revealed from Radar and Surface Mesonetwork Data Analysis. Jess Charba and Yoshikazu Sasaki. October 1968. (PB-183310)

No. 42 A Rainfall Rate Sensor. Brian E. Morgan. November 1968. (PB-183979)

No. 43 Detection and Presentation of Severe Thunderstorms by Airborne and Ground-Based Radars: A Comparative Study. Kenneth E. Wilk, John K. Carter, and J. T. Dooley. February 1969. (PB-183572)

No. 44 A Study of a Severe Local Storm of 16 April 1967. George Thomas Haglund. May 1969. (PB-184-970)

No. 45 On the Relationship Between Horizontal Moisture Convergence and Convective Cloud Formation. Horace R. Hudson. March 1970. (PB-191720)

No. 46 Severe Thunderstorm Radar Echo Motion and Related Weather Events Hazardous to Aviation Operations. Peter A. Barclay and Kenneth E. Wilk. June 1970. (PB-192498)

No. 47 Evaluation of Roughness Lengths at the NSSL-WKY Meteorological Tower. Leslie D. Sanders and Allen H. Weber. August 1970. (PB-194587)

No. 48 Behavior of Winds in the Lowest 1500 ft in Central Oklahoma: June 1966 - May 1967. Kenneth C. Crawford and Horace R. Hudson. August 1970.

No. 49 Tornado Incidence Maps. Arnold Court. August 1970. (COM-71-00019)

No. 50 The Meteorologically Instrumented WKY-TV Tower Facility. John K. Carter. September 1970. (COM-71-00108)

No. 51 Papers on Operational Objective Analysis Schemes at the National Severe Storms Forecast Center. Rex L. Inman. November 1970. (COM-71-00136)

No. 52 The Exploration of Certain Features of Tornado Dynamics Using a Laboratory Model. Neil B. Ward. November 1970. (COM-71-00139)

No. 53 Rawinsonde Observation and Processing Techniques at the National Severe Storms Laboratory. Stanley L. Barnes, James H. Henderson and Robert J. Ketchum. April 1971.

No. 54 Model of Precipitation and Vertical Air Currents. Edwin Kessler and William C. Bumgarner. June 1971.

No. 55 The NSSL Surface Network and Observations of Hazardous Wind Gusts. Operations Staff. June 1971.

No. 56 Pilot Chaff Project at the National Severe Storms Laboratory. Edward A. Jessup. November 1971.

No. 57 Numerical Simulation of Convective Vortices. Robert P. Davies-Jones and Glenn T. Vickers. November 1971.

No. 58 The Thermal Structure of the Lowest Half Kilometer in Central Oklahoma: December 9, 1966 - May 31, 1967. R. Craig Goff and Horace R. Hudson. July 1972.